Available online at www.sciencedirect.com
ScienceDirect
Journal of the European Ceramic Society 29 (2009) 773–777
www.elsevier.com/locate/jeurceramsoc

Energetics of point defects in TiC

Denis Music [a,*], Daniel P. Riley [b], Jochen M. Schneider [a]

[a] *Materials Chemistry, RWTH Aachen University, Kopernikusstr. 16, D-52074 Aachen, Germany*
[b] *Department of Mechanical Engineering, School of Engineering, The University of Melbourne, Victoria 3010, Australia*

Received 9 May 2008; received in revised form 26 June 2008; accepted 27 June 2008

Abstract

Density functional theory was used to evaluate the energetics of point defects in TiC_x ($x<1$): C vacancies and Al substitution at a C site. Our ambition is to contribute towards understanding the underlying atomic mechanisms enabling the Al intercalation into TiC_x and the subsequent formation of Ti_3AlC_2. The difference between the energy of formation for an Al substitution at a C site and a bulk C vacancy is 0.224 eV. Furthermore, only 49 meV/vacancy is required to order the existing bulk C vacancies. Surface effects were also considered: the energy of formation for Al on TiC(1 0 0) at a vacant surface C site is smaller by 2.779 eV than in the case of the C surface vacancy, indicating that Al is likely to be incorporated. Based on these energy differences, it is reasonable to assume that Ti_3AlC_2 is formed by Al surface ingress into TiC_x and that vacancy ordering takes place.

Keywords: Carbides; Defects; Density functional theory

1. Introduction

Intercalation may be defined as the reversible inclusion of an atom or a molecule between two crystalline planes or two other molecules.[1–6] Intercalation is of relevance in solid-state physics and chemistry as well as molecular biology. For instance, many compounds, such as graphite,[1,2] some oxides and sulphides (e.g. V_2O_5 and MoS_2)[3] as well as various clays,[5] possess an enhanced stability and electrical conductivity upon intercalation and can be used in rechargeable lithium batteries, for oil logging, in paper manufacturing and catalysis, to name but a few applications. Magnetic properties can also be altered. For instance, in Ni_3Al the Curie temperature can be tailored by intercalating with carbon.[4] Intercalation of, e.g. daunomycin, ethidium bromide, novantrone and proflavine[6] in DNA is used for chemotherapeutic treatments in medicine. Recently, it has been suggested that bulk synthesis time and temperature of Ti_3AlC_2 can significantly be reduced if a rapid intercalation process route is followed.[7] However, the energetics of underlying atomic mechanisms is not understood.

Ti_3AlC_2 is a so-called $M_{n+1}AX_n$ phase (space group $P6_3/mmc$). These phases are interleaved compounds comprising of $M_{n+1}X_n$ and A layers, where M is an early transition metal, A is mainly IIIA or IVA group element, X is C or N and n is an integer value.[8–10] Due to this nanolaminated structure, these phases exhibit a combination of properties, usually associated with metals and ceramics; they are machinable, possess high stiffness, good thermal shock resistance, good corrosion resistance and they are good conductors of heat and electricity.[8] $M_{n+1}AX_n$ phases are used as formers for healthcare products, hot pressing tools and resistance heating elements.[11,12] Ti_3SiC_2-based composites with Ag or Cu show a potential for electrical contact applications.[13–16] A major challenge in processing these nanolaminates is a reduced synthesis temperature. For instance, Ti_3AlC_2 can be grown at 1400–1600 °C by hot isostatic pressing[17] or by solid–liquid reaction synthesis and simultaneous *in situ* hot pressing process.[18] Riley and Kisi have demonstrated that Ti_3AlC_2 can be synthesised by the rapid intercalation of Al in $TiC_{0.67}$ (space group $Fm\bar{3}m$) at 400–600 °C below the conventional processing temperature.[7] The authors have suggested that, after the ingress of molten Al into $TiC_{0.67}$, vacancy ordering facilitates the formation of Ti_3AlC_2.[7]

In this work, we study the energetics of point defects at a C site in TiC_x ($x<1$): C vacancies and Al substitution at a C site. Our ambition is to contribute towards the understanding of

* Corresponding author. Tel.: +49 2418025972; fax: +49 2418022295.
E-mail address: music@mch.rwth-aachen.de (D. Music).

0955-2219/$ – see front matter © 2008 Elsevier Ltd. All rights reserved.
doi:10.1016/j.jeurceramsoc.2008.06.027

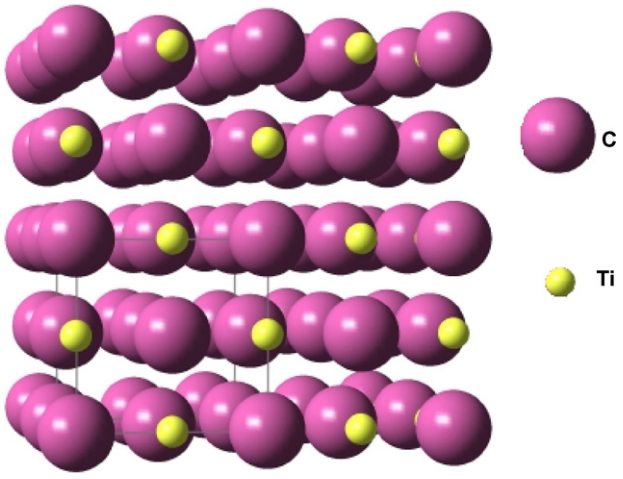

Fig. 1. $2 \times 2 \times 2$ TiC supercell (64 atoms) used in this work. The TiC unit cell (space group $Fm\bar{3}m$) is depicted with solid lines.

atomic mechanisms enabling the rapid intercalation of Al into TiC_x and the subsequent formation of Ti_3AlC_2[7] and $M_{n+1}AX_n$ phases in general. The difference between the energy of formation for an Al substitution at a C site and a bulk C vacancy is 0.224 eV. Surface effects were also considered and we found that the energy of formation for Al on TiC(1 0 0) at a vacant surface C site is smaller by 2.779 eV than in the case of the C surface vacancy, indicating that Al is likely to be incorporated. Based on these energy differences, it is reasonable to assume that the formation of Ti_3AlC_2 is formed by Al surface ingress into TiC_x and C vacancy ordering.

2. Theoretical methods

The theoretical study was carried out using density functional theory,[19] as implemented in the Vienna *ab initio* simulation package (VASP), where the projector augmented wave potentials with the generalized-gradient approximation are employed.[20] The following parameters were applied: convergence criterion for the total energy of 0.01 meV, Blöchl corrections for the total energy,[21] a cut-off of 500 eV, integration in the Brillouin zone according to Monkhorst–Pack[22] with 262,144 grid points in the FFT-mesh and no spin polarization. TiC supercells containing 64 atoms, as shown in Fig. 1, were relaxed with respect to atomic positions and cell volumes. This supercell size was chosen based on the test trials having the requirement of fully containing all local relaxation effects of a vacancy or a substitution. Bulk moduli were obtained by fitting the energy–volume curves using the Birch–Murnaghan equation of states.[23] Energy of formation (E_V or E_S) for the vacancy or Al substitution at a C site, respectively, was calculated as follows:

$$E_V = \frac{E_{TiC,V(C)} + nE_C - E_{TiC}}{n},$$
$$E_S = \frac{E_{TiC,S(Al)} + nE_C - E_{Al} - E_{TiC}}{n} \quad (1)$$

where $E_{TiC,V(C)}$, E_C, E_{TiC}, $E_{TiC,S(Al)}$ and E_{Al} are the total energy of TiC with n C vacancies, the total energy of isolated C (broken periodic boundary conditions), the total energy of the defect-free TiC, the total energy of TiC with an Al substitution at a C site and the total energy of isolated Al (broken periodic boundary conditions), respectively. This procedure was used for describing the energetics of both bulk and surface point defects. Local lattice relaxations relative to the defect site in TiC were obtained using:

$$R_n = \frac{\Delta d_{ij}}{d_{ij}^0} \quad (2)$$

where Δd_{ij} and d_{ij}^0 are the bond length difference and the original bond length, respectively. In order to shed some light on mobility of Al in bulk TiC, its migration energy was calculated. There are several possible pathways for Al to move to a neighbouring vacant site. Hence, we identified a saddle point in the plane perpendicular to the shortest path. The migration energy for Al in [1 1 0] direction was calculated by evaluating the energy difference between the stepwise displaced Al and the supercell with Al at its ideal site. In this procedure, Al was always quenched at its displaced position while all other atoms were fully relaxed.

3. Results and discussion

Table 1 contains the calculated data of the lattice parameters, the bulk moduli and the energy of formation for the point defects in TiC. The following bulk configurations were investigated: (i) one C vacancy, (ii) three C vacancies dispersed in the TiC lattice [(0,0,0), (1/4,3/4,0), (1/4,1/4,1/2)], (iii) three C vacancies ordered along the [1 1 0] direction [(0,0,0), (1/4,1/4,0), (1/2,1/2,0)] as well as (iv) one Al substitution at a C site. The calculated lattice parameter for TiC is 0.2% larger than the experimental value[24] and hence is in good agreement. As C vacancies are introduced, there is no significant change in the lattice parameter. On the other hand, introducing an Al substitution in the TiC_x lattice ($x < 1$) at the C site causes an increase of the lattice parameter by 0.6%, which may be explained by the larger size of Al as compared to C. The calculated bulk modulus for pure TiC is 12.1% larger than the experimentally obtained value,[25] which is within the expected deviation for the exchange-correlation approximation used here. Minor changes in the bulk moduli are observed when C vacancies or an Al substitution

Table 1
Calculated lattice parameters (a), bulk moduli (B), and energy of formation (E_V or E_S) for the C vacancy or Al substitution at a C site in bulk and surface TiC

	a (Å)	B (GPa)	E_V or E_S (eV/defect)
TiC	4.338	265	–
TiC–vacancy (single), bulk	4.338	260	9.916
TiC–vacancy (single), (1 0 0) surface	–	–	9.763
TiC–vacancy (triple)			
Bulk			
Ordered	4.339	251	10.072
Dispersed	4.339	251	10.023
TiC–Al substitution, bulk	4.366	254	10.140
TiC–Al substitution, (1 0 0) surface	–	–	6.984

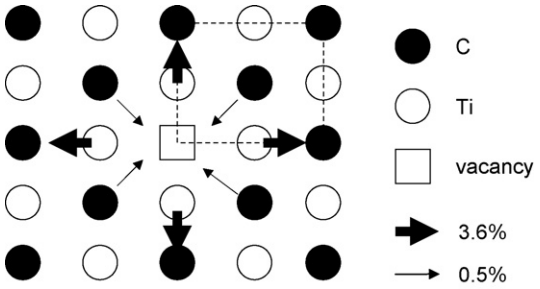

Fig. 2. Local lattice relaxations, as indicated by arrows, in bulk TiC_x induced by the presence of a C vacancy. The (1 0 0) plane of the TiC supercell is shown.

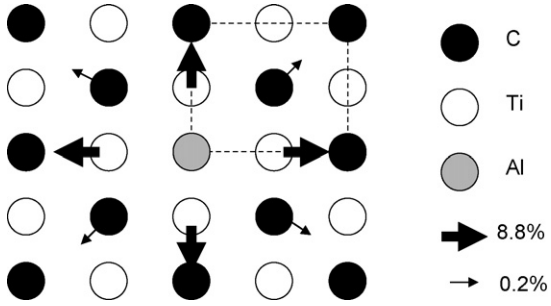

Fig. 3. Local lattice relaxations, as indicated by arrows, in bulk TiC_x induced by an Al substitution. The (1 0 0) plane of the TiC supercell is shown.

are introduced into TiC. The calculated energy of formation for a single C vacancy or an Al substitution at a C site is 9.916 and 10.140 eV, respectively. When three C vacancies are introduced to form an ordered cluster along the [1 1 0] direction or they are dispersed in the TiC_x lattice, the energies of formation are 10.072 and 10.023 eV/vacancy, respectively. These vacancy formation values in TiC_x are comparable with the data obtained for nitrogen vacancies in Ti_4AlN_3[26] and oxygen vacancies in HfO_2 and SiO_2.[27] Furthermore, Hugosson et al. have calculated the energy of formation for TiC and TiC_x ($x < 1$) with respect to the elements and reported that TiC is by 1–15 meV/atom more stable than $TiC_{0.9375}$,[28] which is in agreement with our vacancy formation data. The difference between the energy of formation for an Al substitution at a C site and a bulk C vacancy is 0.224 eV, suggesting that Al may be incorporated into the TiC_x lattice, because the magnitude of this energy difference is comparable to the energy required to form metastable cubic $Ti_{1-x}Al_xN$[29] and Cu–Mo[30] by vapour phase condensation. Furthermore, it appears that only 49 meV/vacancy is required to order the C vacancies. Based on these minute energy differences, it is reasonable to assume that the formation of Ti_3AlC_2 is accomplished by Al ingress into TiC_x and C vacancy ordering as previously suggested by Riley and Kisi.[7] At temperatures of approximately 1000–1100 °C in vacuum, it has previously been reported that Ti_3SiC_2 rapidly decomposes into TiC_x and Si by egress of Si from the A-site to the crystallite surface and subsequent evaporation.[31] This is in principle a reverse intercalation process. Hence, our intercalation data may also be relevant to describe decomposition.

Another important aspect of the C vacancy formation and the Al substitution are the local lattice relaxations. Fig. 2 shows the local lattice relaxations in the (1 0 0) plane induced by the presence of a C vacancy. The nearest neighbours (Ti atoms in the first coordination shell) move outwards by 3.6%. The second nearest neighbours (C atoms in the second coordination shell) move inwards by 0.5%. There are no local lattice relaxations found in higher coordination shells, which implies that the chosen supercell size is adequate. These local lattice relaxations are consistent with a previously reported *ab initio* study[28] and neutron diffraction data.[32] In the case of three C vacancies in the TiC lattice, similar local lattice relaxations are observed. For the ordered C vacancies, the nearest neighbours move outwards by 3.3–3.7%, while in the case of dispersed C vacancies, the nearest neighbours move outwards by 3.9–4.1%. As Al is introduced onto the C site, the local lattice relaxations differ from those of a purely vacant site. Fig. 3 shows the local lattice relaxations in the (1 0 0) plane induced by the Al substitution. Both the first and the second coordination shells exhibit the outward relaxation with values of 8.8% and 0.2%, respectively. The third coordination shell remains unaffected. This can be understood based on the same rationale as in the case of the lattice parameter data discussed above. Al is larger in size than C so that only outward local lattice relaxations can be expected. These local structural relaxations may be a prerequisite for the migration of Al in TiC_x.

As suggested above, it is reasonable to assume that Al substitutes C in the TiC_x lattice which can accommodate large enough local lattice relaxations. It remains to explore if Al can diffuse in the TiC_x lattice and therefore we calculate the migration energy for Al in the [1 1 0] direction. We chose to investigate this particular pathway based on self-diffusion study,[33] identifying this path as a migration pathway for NaCl type lattices. Fig. 4 shows the schematics of Al migration in TiC_x bulk. Al moves in the [1 1 0] direction to a neighbouring vacant site and it is expected that the saddle point is reached when both x and y reduced coordinates are 0.125. Fig. 5 shows the energetics of this migration. Two maxima (saddle points) are observed, belonging to (I) a tetrahedral interstitial position with the potential barrier of 0.05 eV and (II) to octahedral vacancy (C site) position with the potential barrier of 0.82 eV. These maxima are highlighted in Fig. 5. Yttria-stabilized zirconia is a well-known ionic conductor and the migration energy of oxygen in this structure was reported to be in the range from 0.20 to 1.40 eV,[34] which is comparable with our data. Fig. 6 shows the displacement of the nearest neighbours of Al during migration in the [1 1 0] direction. These values are consistent with literature.[35] Based on these data, we suggest that Al moves thermally activated in the TiC_x lattice if C

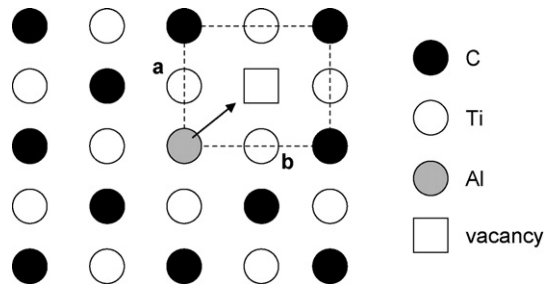

Fig. 4. Migration of Al in bulk TiC_x. The (1 0 0) plane of the TiC supercell is shown. Two nearest neighbours (a and b) are highlighted.

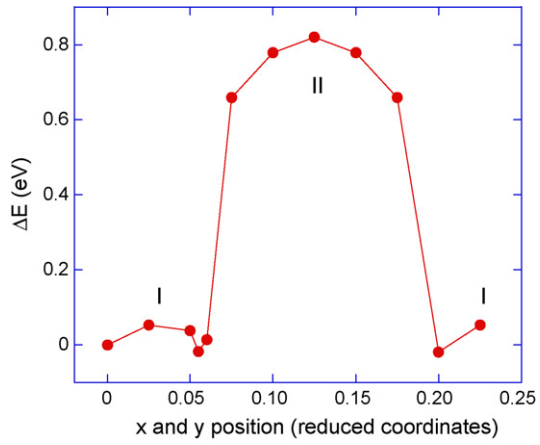

Fig. 5. Migration energy (ΔE) for Al in the [1 1 0] direction of TiC_x. Two saddle points are marked with Roman numerals.

vacancies are present. This is consistent with the experimentally reported formation of Ti_3AlC_2 from $TiC_{0.67}$ and molten Al.[7]

To identify the atomic mechanisms active during the initial stages of the Ti_3AlC_2 formation, we analyse the Al/TiC_x interface. We calculate the energetics of a C vacancy and an Al substitution at a vacant C site on the TiC(1 0 0) surface. Depending on film deposition conditions, TiN grows with 0 0 1- or 1 1 1-texture.[36] Since TiN and TiC are isostructural, we chose to study TiC(1 0 0) surface in this work. The calculated energies of formation for a C vacancy or the Al substitution are 9.763 and 6.984 eV, respectively (see Table 1). The energy of formation for a C vacancy on the (1 0 0) surface was calculated to be 0.153 eV smaller than a vacancy within bulk TiC_x. This can be understood based on the so-called broken-bond model[37,38]; it can be expected that the energy penalty is smaller when less bonds are broken as is the case during formation of a surface vacancy. As Al is introduced into the TiC_x lattice at a C vacancy site, the energy of formation is smaller by 2.779 eV for a (1 0 0) surface site. This is again consistent with the broken-bond model[37,38] as less bonds are broken so that this scenario represents the smallest energy penalty. Simultaneously, surface sites allow for larger local lattice relaxations required to incorporate Al into TiC_x. Both arguments indicate that the incorporation probability of Al at the Al/TiC_x interface during bulk synthesis or during vapour phase condensation is high. It is reasonable to assume that the intercalation kinetics depends not only on vacancy ordering but also on the grain-boundary-to-volume ratio. These data may also be relevant for modelling the structure evolution during vapour phase condensation. During high temperature magnetron sputtering the formation of a binary transition metal carbide buffer layer is often reported.[39] It may be speculated that $M_{n+1}AX_n$ phase nucleation may occur at this interface by intercalation during vapour phase condensation. Previously, we have shown that M_2AlC phases can be classified into two groups according to the valence electron concentration of the transition metal M: weakly coupled (M = Sc, Ti, Zr, Hf) and strongly coupled (M = V, Nb, Ta, Cr, Mo, W) nanolaminates.[40–43] This notion is based on coupling between MC and Al[40–42] as well as MC and MC layers.[43] The cause for coupling is the bond energy difference between M–C and M–A.[44] The results obtained in this work may be of general relevance for the formation of $M_{n+1}AX_n$ phases with similar bond energy differences between M–X and M–A bonds like in the Ti–Al–C system.

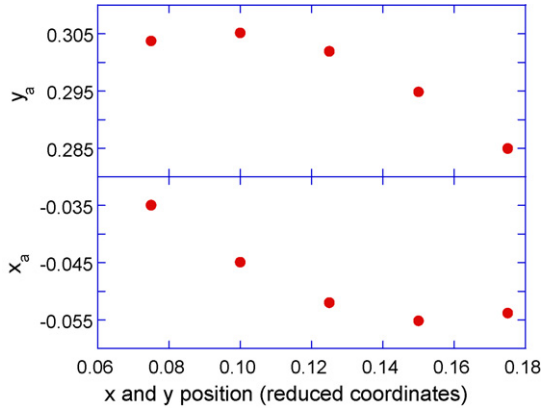

Fig. 6. Displacement of the nearest neighbours (a or b) of Al during migration in the [1 1 0] direction of TiC_x.

4. Conclusions

We have used *ab initio* calculations to evaluate the energetics of point defects in TiC_x ($x < 1$). Two point defects were considered: C vacancy and Al substitution at the vacant C site. Our ambition is to better understand the underlying atomic mechanisms enabling the intercalation of Al into TiC_x to synthesise Ti_3AlC_2.[7] The difference between the energy of formation for an Al substitution at a C site and a bulk C vacancy is low at 0.224 eV, suggesting that Al may readily be incorporated into TiC_x. Furthermore, only 49 meV/vacancy is required to order the C vacancies. The migration energy of Al in the [1 1 0] direction is 0.82 eV, which implies that Al migration in the TiC_x lattice is likely to occur. Surface effects were also considered in this work and we found that the energy of formation for Al on TiC(1 0 0) at a vacant surface C site is by 2.779 eV smaller than in the case of the C surface vacancy, indicating that Al is likely to be incorporated. Based on these energy differences, it is reasonable to assume that Ti_3AlC_2 is formed through surface ingress of Al into TiC_x, aided by the ordering of C vacancies.

Acknowledgements

Effort sponsored by the Air Force Office of Scientific Research, Air Force Material Command, USAF, under grant number FA8655-07-1-3052. The U.S. Government is authorized to reproduce and distribute reprints for Government purpose notwithstanding any copyright notation thereon. Additional funding support was provided by the Australian Institute of Nuclear Science and Technology (AINSE Fellowship).

References

1. Boehm, H.-P., Setton, R. and Stumpp, E., Nomenclature and terminology of graphite-intercalation compounds (IUPAC recommendations 1994). *Pure Appl. Chem.*, 1994, **66**(9), 1893–1901.

2. Katinonkul, W. and Lerner, M. M., Graphite intercalation compounds with large fluoroanions. *J. Fluorine Chem.*, 2007, **128**(4), 332–335.
3. Julien, C. M., Lithium intercalated compounds—charge transfer and related properties. *Mater. Sci. Eng. R*, 2003, **40**(2), 47–102.
4. Tong, P., Zhu, X. B., Zhao, B. C., Ang, R., Song, W. H. and Sun, Y. P., Influence of carbon intercalation on the structure and magnetic properties of Ni_3Al. *Physica B*, 2006, **371**(1), 63–67.
5. Solin, S. A., Clays and clay intercalation compounds: properties and physical phenomena. *Annu. Rev. Mater. Sci.*, 1997, **27**, 89–115.
6. Kostjukov, V. V., Lantushenko, A. O., Davies, D. B. and Evstigneev, M. P., On the origin of the decrease in stability of the DNA hairpin d(GCGAAGC) on complexity with aromatic drugs. *Biophys. Chem.*, 2007, **129**(1), 56–59.
7. Riley, D. P. and Kisi, E. H., The design of crystalline precursors for the synthesis of $M_{n+1}AX_n$ phases and their application to Ti_3AlC_2. *J. Am. Ceram. Soc.*, 2007, **90**(7), 2231–2235.
8. Barsoum, M. W., The $M_{n+1}AX_n$ phases: a new class of solids; Thermodynamically stable nanolaminates. *Prog. Solid State Chem.*, 2000, **28**(1–4), 201–281.
9. Music, D. and Schneider, J. M., The correlation between the electronic structure and elastic properties of nanolaminates. *JOM*, 2007, **59**(7), 60–64.
10. Lin, Z. J., Li, M. S. and Zhou, Y. C., TEM investigations on layered ternary ceramics. *J. Mater. Sci. Technol.*, 2007, **23**(2), 145–165.
11. www.3one2.com.
12. www.kanthal.com.
13. Eklund, P., Emmerlich, J., Högberg, H., Wilhelmsson, O., Isberg, P., Birch, J. *et al.*, Structure, electrical and mechanical properties of nc-TiC/a-SiC nanocomposite thin films. *J. Vac. Sci. Technol. B*, 2005, **23**(6), 2486–2495.
14. Emmerlich, J., Eklund, P., Högberg, H. and Hultman, L., Electrical resistivity of $Ti_{n+1}AC_n$ (A = Si, Ge, Sn, n = 1–3) thin films. *J. Mater. Res.*, 2007, **22**(8), 2279–2287.
15. Eklund, P., Joelsson, T., Ljungcrantz, H., Wilhelmsson, O., Czigány, Zs., Högberg, H. *et al.*, Microstructure and electrical properties of Ti–Si–C–Ag nanocomposite thin films. *Surf. Coat. Technol.*, 2007, **201**(14), 6465–6469.
16. Zhang, J., Wang, J. Y. and Zhou, Y. C., Structure stability of Ti_3SiC_2 in Cu and microstructure evolution of Cu–Ti_3SiC_2 composites. *Acta Mater.*, 2007, **55**(13), 4381–4390.
17. Tzenov, N. V. and Barsoum, M. W., Synthesis and characterization of Ti_3AlC_2. *J. Am. Ceram. Soc.*, 2000, **83**(4), 825–832.
18. Wang, X. H. and Zhou, Y. C., Microstructure and properties of Ti_3AlC_2 prepared by the solid-liquid reaction synthesis and simultaneous in-situ hot pressing process. *Acta Mater.*, 2002, **50**(12), 3141–3149.
19. Hohenberg, P. and Kohn, W., Inhomogeneous electron gas. *Phys. Rev.*, 1964, **136**(3B), B864–B871.
20. Kresse, G. and Joubert, D., From ultrasoft pseudopotentials to the projector augmented-wave method. *Phys. Rev. B*, 1999, **59**(3), 1758–1775.
21. Blöchl, P. E., Projector augmented-wave method. *Phys. Rev. B*, 1994, **50**(24), 17953.
22. Monkhorst, H. J. and Pack, J. D., Special points for Brillouin-zone integrations. *Phys. Rev. B*, 1976, **13**(12), 5188–5192.
23. Birch, F., Finite strain isotherm and velocities for single-crystal and polycrystalline NaCl at high-pressures and 300-degree-K. *J. Geophys. Res.*, 1978, **83**(NB3), 1257–1268.
24. Zee, R., Yang, C., Lin, Y. X. and Chin, B., Effects of boron and heat-treatment on structure of dual-phase Ti–TiC. *J. Mater. Sci.*, 1991, **26**(14), 3853–3861.
25. Dodd, S. P., Cankurtaran, M. and James, B., Ultrasonic determination of the elastic and nonlinear acoustic properties of transition-metal carbide ceramics: TiC and TaC. *J. Mater. Sci.*, 2003, **38**(6), 1107–1115.
26. Music, D., Ahuja, R. and Schneider, J. M., Theoretical study of nitrogen vacancies in Ti_4AlN_3. *Appl. Phys. Lett.*, 2005, **86**(3), 031911.
27. Scopel, W. L., da Silva, A. J. R., Orellana, W. and Fazzio, A., Comparative study of defect energetics in HfO_2 and SiO_2. *Appl. Phys. Lett.*, 2004, **84**(9), 1492–1494.
28. Hugosson, H. W., Korzhavyi, P., Jansson, U., Johansson, B. and Eriksson, O., Phase stability and structural relaxations in substoichiometric TiC_{1-x}. *Phys. Rev. B*, 2001, **63**(16), 165116.
29. Mayrhofer, P. H., Music, D. and Schneider, J. M., Influence of the Al distribution on the structure, elastic properties, and phase stability of supersaturated $Ti_{1-x}Al_xN$. *J. Appl. Phys.*, 2006, **100**(9), 094906.
30. Gong, H. R., Kong, L. T. and Liu, B. X., Metastability of an immiscible Cu–Mo system calculated from first-principles and a derived n-body potential. *Phys. Rev. B*, 2004, **69**(2), 024202.
31. Emmerlich, J., Music, D., Eklund, P., Wilhelmsson, O., Jansson, U., Schneider, J. M. *et al.*, Thermal stability of Ti_3SiC_2 thin films. *Acta Mater.*, 2007, **55**(4), 1479–1488.
32. Moisy-Maurice, V., de Novion, C. H., Christensen, A. N. and Just, W., Elastic diffuse neutron-scattering study of the defect structure of $TiC_{0.67}$ and $NbC_{0.73}$. *Solid State Commun.*, 1981, **39**(5), 661–665.
33. Oshcherin, B. N., Enthalpy of activation for self-diffusion of inorganic substances having the NaCl structure. *Rus. Phys. J.*, 1972, **12**(9), 1224–1227.
34. Pornprasertsuk, R., Ramanarayanan, P., Musgrave, C. B. and Prinz, F. B., Predicting ionic conductivity of solid oxide fuel cell electrolyte from first principles. *J. Appl. Phys.*, 2005, **98**(10), 103513.
35. Mercer, J. L., Nelson, J. S., Wright, A. F. and Stechel, E. B., Ab initio calculations of the energetics of the neutral Si vacancy defect. *Model. Simul. Mater. Sci. Eng.*, 1998, **6**(1), 1–8.
36. Gall, D., Kodambaka, S., Wall, M. A., Petrov, I. and Greene, J. E., Pathways of atomistic processes on TiN(0 0 1) and (1 1 1) surfaces during film growth: an *ab initio* study. *J. Appl. Phys.*, 2003, **93**(11), 9086–9094.
37. Bragg, W. L. and Williams, E. J., The effect of thermal agitation on atomic arrangement in alloys. *Proc. R. Soc. Lond. Ser. A*, 1934, **145**, 699–730.
38. Becker, R., *Ann. Phys.*, 1938, **32**, 128–140.
39. Högberg, H., Hultman, L., Emmerlich, J., Joelsson, T., Eklund, P., Molina-Aldareguia, J. M. *et al.*, Growth and characterization of MAX-phase thin films. *Surf. Coat. Technol.*, 2005, **193**(1–3), 6–10.
40. Music, D., Sun, Z. M., Ahuja, R. and Schneider, J. M., Coupling in nanolaminated ternary carbides studied by theoretical means: the influence of electronic potential approximations. *Phys. Rev. B*, 2006, **73**(13), 134117.
41. Sun, Z. M., Music, D., Ahuja, R., Li, S. and Schneider, J. M., Bonding and classification of nanolayered ternary carbides. *Phys. Rev. B*, 2004, **70**(9), 092102.
42. Music, D., Sun, Z. M. and Schneider, J. M., Electronic structure of Sc_2AC (A = Al, Ga, In, Tl). *Solid State Commun.*, 2005, **133**(6), 381–383.
43. Music, D., Sun, Z. M., Voevodin, A. A. and Schneider, J. M., Electronic structure and shearing in nanolaminated ternary carbides. *Solid State Commun.*, 2006, **139**(4), 139–143.
44. Music, D., Houben, A., Dronskowski, R. and Schneider, J. M., Ab initio study of ductility in M_2AlC (M = Ti, V, Cr). *Phys. Rev. B*, 2007, **75**(17), 174102.